49th IEEE Conference on Decision and Control
December 15-17, 2010
Hilton Atlanta Hotel, Atlanta, GA, USA

Underactuated Control and Distribution of Multi-Agent Systems in Stratified Flow Environments

Robert H. Krohn and Thomas R. Bewley

Abstract— **The present paper shows how vertical actuation alone may be used to effectively control the spatial distribution of mobile vehicles ("balloons" in air, or "drifters" in water) in vertically-stratified background flows. Applying iterative, adjoint-based, model predictive control (MPC) techniques coupled with linear quadratic regular (LQR) feedback, agent trajectories and feedback control strategies are determined to ensure the desired terminal-time spacing of multiple agents. Variations in both starting locations and disturbances are considered to illustrate the significant control authority in this agent separation problem in both laminar and turbulent background flows, despite the fact that linear controllability is lost in certain limiting cases. The paper thus demonstrates a novel application of feedback control theory to an emerging real-world application in multi-agent systems. The results lay the groundwork for future applications in Lagrangian sampling of underwater ecosystems as well as the efficient sampling of hurricanes for the purpose of forecasting their development.**

I. Introduction

Studies of both oceanic and atmospheric currents via Lagrangian motions have been widely documented and used for modeling and research [1] [2]. Historically, these methods have relied on passive motion of buoyant vehicles, but more recently drifters with controllable buoyancy have been used to perform Lagrangian and mass-transport studies, such as the international Argo Project [1] deployed to monitor ocean currents on a global scale. Recent work by the atmospheric research community has established the capability of actively and efficiently altering the internal density of a balloon, thus enabling buoyancy control in the atmosphere over extended periods of time [2]. The ability to actively change buoyancy (and, thus, vertical position) in such strongly stratified flow systems opens the door to a host of interesting new low-power topology control problems.

The key idea of the multi-agent coordinated control strategy proposed in this work is to leverage the stratification of the flow environment in order to establish and maintain a degree of control over the topology of the swarm. Leveraging nonlinear model predictive control (MPC) and the linear quadratic regulator (LQR), new methods for the active control of the spatial distribution of several such buoyancy-actuated agents have been developed.

This buoyancy-control-in-stratified-flow approach extends naturally to underwater vehicles in coastal systems, as the coastal ocean is also characterized by a flow field with significant variability in both space and time.

II. Background

To begin, the background stratified flow (Fig. 1) is taken as a simple pressure-driven (Poiseuille) flow between two

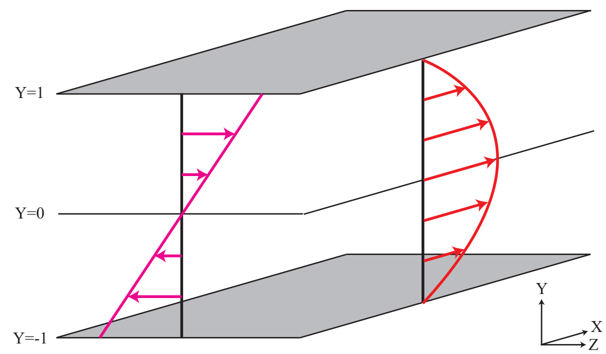

Fig. 1. Flow velocities of the basic flow considered in this paper, which is pressure-driven in the x direction and shear driven in the z direction.

impermeable infinite plates with no-slip boundaries in the streamwise direction x, shear-driven (Couette) flow in the spanwise direction z, and no flow in the vertical direction y. The channel half-width and maximum flow velocity in x and z are rescaled to unity without loss of generality.

Starting from this physical description of the flow system in Cartesian coordinates, the state of each agent is defined as its position in 3-space relative to an arbitrarily-chosen origin in the streamwise and spanwise directions, and the channel centerline in the vertical direction. Mathematically, the agent forcing terms (non-dimensional relative velocities) can then be described as a functions of the vertical position, y, and the vertical velocity, f; that is, for the i'th agent:

$$\frac{d}{dt}\begin{bmatrix} x_i \\ y_i \\ z_i \end{bmatrix} = \begin{bmatrix} -{y_i}^2+1 \\ f_i \\ y_i \end{bmatrix}, \tag{1}$$

where f is defined as the system input. It is assumed that the vertical actuation of the agent occurs sufficiently quickly, relative to the speed of the background flow, that the agent can move vertically (within the vertical confines of the channel) before moving significantly in the streamwise or spanwise directions (stated another way, we assume that the channel half-width is small with respect to the horizontal distances of interest). This simplification of the background flow retains the stratified nature of many natural flows, and presents enough nonlinear characteristics in the model to make the problem interesting, difficult, and relevant in the consideration of harder problems in the environment.

In the interest of uniform sampling, we focus on the relative separation of agents throughout the volume, rather than the individual location of each agent in absolute coordinates. We thus turn our attention to begin with the relative

978-1-4244-7746-3/10/$26.00 ©2010 IEEE

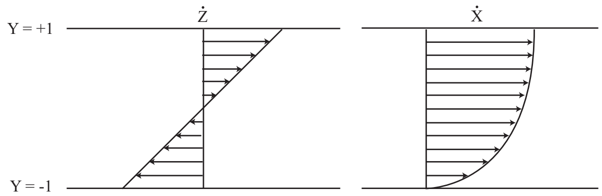

Fig. 2. Flow velocity profiles of an alternative flow configuration [cf. Fig. 1] resulting in the same simplified nonlinear model [compare (4) to (7)].

separation of two such agents.

III. Problem Formulation

As mentioned above, we now focus on two-agent systems, $i = [1,2]$, and the agent distribution is described in terms of the relative horizontal separation of these two agents. We thus introduce a change of variables (COV) which focuses specifically on this separation. Starting from the initial state variables introduced in (1), and introducing the specified separation target distances C_x and C_z, two new COV states $\hat{x}$ and $\hat{y}$ are defined such that:

$$\hat{x} \triangleq x_1 - x_2 + C_x, \tag{2a}$$

$$\hat{z} \triangleq z_1 - z_2 + C_z. \tag{2b}$$

Note that $\hat{x} = \hat{z} = 0$ corresponds to the agents being at the specified separation. Now define the intermediate control variables u_1 and u_2 as linear combinations of the agents' vertical positions,

$$\begin{bmatrix} u_1 \\ u_2 \end{bmatrix} \triangleq \begin{bmatrix} -y_1 - y_2 \\ y_1 - y_2 \end{bmatrix}, \tag{3}$$

and take the time derivative of the COV states equation (2), a simple nonlinear description of the agent-separation system is found:

$$\frac{d}{dt}\begin{bmatrix} \hat{x} \\ \hat{z} \end{bmatrix} = \frac{d}{dt}\begin{bmatrix} x_1 - x_2 \\ z_1 - z_2 \end{bmatrix} = \begin{bmatrix} -y_1^2 + y_2^2 \\ y_1 - y_2 \end{bmatrix} = \begin{bmatrix} u_1 u_2 \\ u_2 \end{bmatrix}. \tag{4}$$

Interestingly, the nonlinear model given in (4) may also be derived for an alternative flow configuration with a half-parabolic velocity profile in the streamwise direction and a linear velocity profile in the spanwise direction (Fig. 2). In this case, the state equation governing the movement of agents in the system is given by [cf. (1)]:

$$\frac{d}{dt}\begin{bmatrix} x_i \\ y_i \\ z_i \end{bmatrix} = \begin{bmatrix} 2y_i - {y_i}^2 \\ f_i \\ y_i \end{bmatrix}. \tag{5}$$

Using the same COV for the separation of the agents as proposed in (2), redefining the intermediate control variables u_1 and u_2 such that [cf. (3)]

$$\begin{bmatrix} u_1 \\ u_2 \end{bmatrix} \triangleq \begin{bmatrix} 2 - y_1 - y_2 \\ y_1 - y_2 \end{bmatrix}, \tag{6}$$

and following the same differentiation processes as used before, it is again found [cf. (4)] that

$$\frac{d}{dt}\begin{bmatrix} \hat{x} \\ \hat{z} \end{bmatrix} = \begin{bmatrix} 2\,(y_1 - y_2) - y_1^2 + y_2^2 \\ y_1 - y_2 \end{bmatrix} = \begin{bmatrix} u_1 u_2 \\ u_2 \end{bmatrix}. \tag{7}$$

That is, the same nonlinear model is obtained, though the intermediate control variables, u_1 and u_2, are defined differently.

Curiously, linearization of (4) [equivalently, (7)], taking $u_1 = \bar{u}_1 + \bar{u}_1'$, $u_2 = \bar{u}_2 + \bar{u}_2'$, etc., about the nominal solution (with $\bar{u}_1 = \bar{u}_2 = 0$, assuming primed quantities are small) results immediately in the observation that $d\hat{x}'/dt = 0$; that is, $\hat{x}$ is *linearly uncontrollable*. Some finite oscillation of u_2 is required in order to give control authority on $\hat{x}$ via the control variable u_1. This is an immediate indication of the delicateness of the present system. Despite the loss of linear controllability in this limit, it is seen that there is in fact a lot of control authority in this problem if finite vehicle motions are allowed, as explored in the balance of this paper.

For simplicity, the remainder of this paper focuses on the flow described in Figure 1 and modeled in the laminar flow case by (1), with the relevant COV defined by (2) and intermediate control variables defined by (3).

IV. Model Predictive Control

The intermediate control variables u_1 and u_2 are related to the time derivatives of the agent inputs f_1 and f_2; thus, u_1 and u_2 should be kept sufficiently *smooth* such that f_1 and f_2 are sufficiently *small*. By introducing another change of variables, $v_i = du_i/dt$, and penalizing an energy measure of the v_i in the control formulation, this is readily achieved:

$$\frac{d}{dt}\begin{bmatrix} u_1 \\ u_2 \end{bmatrix} = \begin{bmatrix} v_1 \\ v_2 \end{bmatrix} = \begin{bmatrix} -f_1 - f_2 \\ f_1 - f_2 \end{bmatrix}. \tag{8}$$

Finally, the state vector, $\mathbf{q}$, and control vector, $\mathbf{v}$, are defined in order to facilitate the discussion of the relevant state-space formulation of the present problem:

$$\mathbf{q} \triangleq \begin{bmatrix} \hat{x} \\ \hat{z} \\ u_1 \\ u_2 \end{bmatrix}, \quad \mathbf{v} \triangleq \begin{bmatrix} v_1 \\ v_2 \end{bmatrix}. \tag{9}$$

The construction of the change of variables is closely tied to the formulation of an associated cost function, which, when minimized, drives the system to behave in a desired fashion. Using a quadratic model that penalizes state and input values, driving the cost toward 0 keeps physical inputs small and drives agent separation to specified parameters (i.e. $x_2 - x_1 \rightarrow C_x$ and $z_2 - z_1 \rightarrow C_z$).

Thus, the cost function, $J(\mathbf{q},t)$, is defined with a state weighting matrix $Q_{\mathbf{q}}$, input weighting matrix $Q_{\mathbf{v}}$, and terminal-time weighting matrix Q_T:

$$J = \frac{1}{2}\int_0^T \left(\mathbf{q}^T Q_{\mathbf{q}} \mathbf{q} + \mathbf{v}^T Q_{\mathbf{v}} \mathbf{v}\right) dt + \frac{1}{2}\mathbf{q}^T(T)\, Q_T\, \mathbf{q}(T). \tag{10}$$

An input sequence is determined using an adjoint-based iterative optimization technique to minimize the cost function with respect to the input [4] [5]. This iterative scheme creates a model-based predictive controller (MPC), which is solved by a time-based input sequence $\mathbf{v}(t)$ that reduces the cost function over a time window (in this case driving the states toward 0 and minimizing the associated input costs).

Starting from the nonlinear state space equations presented in 4, 8, and 9, the tangent linear equation of the system is found by replacing the state with perturbed state variables (such as $\hat{x} \rightarrow \hat{x}+\hat{x}'$) and solving for the perturbed variables:

$$\frac{d}{dt}\begin{bmatrix}\hat{x}' \\ \hat{z}' \\ u_1' \\ u_2'\end{bmatrix} = \begin{bmatrix}u_2 u_1' + u_1 u_2' \\ u_2' \\ v_1' \\ v_2'\end{bmatrix} \Rightarrow \frac{d\mathbf{q}'}{dt} = A\mathbf{q}' + B\mathbf{v}'. \tag{11}$$

Additionally, doing the same perturbation analysis to the cost function, (10), a small change in the cost can be written

$$J' = \int_0^T \left(\mathbf{q}^T Q_{\mathbf{q}}\mathbf{q}' + \mathbf{v}^T Q_{\mathbf{v}}\mathbf{v}'\right) dt + \mathbf{q}^T(T)\, Q_T \mathbf{q}'(T). \tag{12}$$

This perturbation of the cost function can be defined in terms of a gradient with respect to the system input using an adjoint based analysis. First defining the weighted inner product, $\langle\langle a,b\rangle\rangle \triangleq \int_0^T a^H b dt$, and then using an adjoint identity:

$$\langle\langle \mathbf{r}, \mathcal{L}\mathbf{q}'\rangle\rangle = \langle\langle \mathcal{L}^*\mathbf{r}, \mathbf{q}'\rangle\rangle + b, \tag{13a}$$

which is equivalent to

$$\int_0^T \mathbf{r}^T \mathcal{L}\mathbf{q}' dt = \int_0^T (\mathcal{L}^*\mathbf{r})^T \mathbf{q}' dt + b, \tag{13b}$$

for some, as yet, undefined operator, $\mathcal{L}$, and adjoint variable, $\mathbf{r}$. Then choosing to relate the state with the input by choosing

$$\mathcal{L}\mathbf{q}' = B\mathbf{v}', \tag{14}$$

the operator, $\mathcal{L}$, is found by plugging into (11) and solving to get:

$$\mathcal{L} = \frac{d}{dt} - A. \tag{15}$$

Returning this result to the adjoint identity (13b),

$$\int_0^T \mathbf{r}^T \left(\frac{d\mathbf{r}}{dt} - A\right)\mathbf{q}' dt = \int_0^T (\mathcal{L}^*\mathbf{r})^T \mathbf{q}' dt + b, \tag{16}$$

which can then be integrated by parts

$$\mathbf{r}^T\mathbf{q}'|_0^T - \int_0^T \left(\frac{d\mathbf{r}}{dt} - \mathbf{r}^T A\right)\mathbf{q}' dt = \int_0^T (\mathcal{L}^*\mathbf{r})^T \mathbf{q}' dt + b \tag{17}$$

which means

$$b = \mathbf{r}^T\mathbf{q}'|_0^T \tag{18a}$$

$$\mathcal{L}^*\mathbf{r} = -\left(\frac{d}{dt} + A^T\right)\mathbf{r}. \tag{18b}$$

Plugging Eqs. 14 and 18a into the adjoint identity, (16):

$$\int_0^T \mathbf{r}^T B\mathbf{v}' dt = \int_0^T (\mathcal{L}^*\mathbf{r})^T \mathbf{q}' dt + \mathbf{r}^t\mathbf{q}'|_0^T. \tag{19}$$

Now comparing (19) to the perturbed cost function, (12), and then choosing to define:

$$\mathcal{L}^*\mathbf{r} = Q_{\mathbf{q}}\mathbf{q} \tag{20}$$

and

$$\mathbf{r} = Q_T\mathbf{q} \tag{21}$$

the adjoint identity is again re-written:

$$\begin{aligned}\textstyle\int_0^T \mathbf{r}^T B\mathbf{v}' dt &= \textstyle\int_0^T (Q_{\mathbf{q}}\mathbf{q})^T \mathbf{q}' dt + (Q_T\mathbf{q})^T \mathbf{q}' \\ &= \textstyle\int_0^T \mathbf{q}^T Q_{\mathbf{q}}\mathbf{q}' dt \mathbf{q}^T Q_T \mathbf{q}'.\end{aligned} \tag{22}$$

This means that the prerturbed cost function can then be written in terms of the left-hand-side of (22), resulting in a description of the cost function as an equation of a perturbation of the system input, $\mathbf{v}'$, and the adjoint variable, $\mathbf{r}$:

$$J' = \int_0^T \left[B^T\mathbf{r} + Q_{\mathbf{v}}\mathbf{v}\right]\mathbf{v}' dt. \tag{23}$$

Which leads to, via the definition of the inner product, a gradent of the cost function with respect to the system in put as a differential equation of the form:

$$J' = \langle\langle \frac{\mathcal{D}J}{\mathcal{D}\mathbf{v}}, \mathbf{v}'\rangle\rangle \quad \text{where} \quad \frac{\mathcal{D}J}{\mathcal{D}\mathbf{v}} = B^T\mathbf{r} + Q_{\mathbf{v}}\mathbf{v}. \tag{24}$$

Resolving the definition of the adjoint variable, $\mathbf{r}$, (18) is combined with the chosed values of Eqs. 18b and 21 such that:

$$\begin{gathered}\mathcal{L}^*\mathbf{r} = Q_{\mathbf{v}}\mathbf{r} \Leftrightarrow -\tfrac{d\mathbf{r}}{dt} = A^H\mathbf{r} + Q_{\mathbf{v}}\mathbf{v} \\ \text{for} \quad 0 < t < T,\end{gathered} \tag{25a}$$

which is subject to the 'initial' conditions:

$$\mathbf{r} = Q_T\mathbf{q} \quad \text{at} \quad t = T. \tag{25b}$$

Starting from the terminal definition of the adjoint field, $\mathbf{r} = Q_T\mathbf{q}$, the gradient is determined via a backwards march, from $t = T \rightarrow 0$, using an RK4 march.

Using a conjugate gradient descent method, in conjunction with a Brent line search, a descent direction and a step size are found. Moving the input 'downhill' creates a new input sequence, which is then used to determine a new, lower cost, trajectory path which can form the basis of the next minimization iteration.

Upon satisfaction of a prescribed convergence criteria, the resultant COV input sequence, $\mathbf{v}(t)$, satisfies a local minimization of the cost function. Using this sequence and the invertible relationship found in (8), the physical agent input sequences, $f_1(t)$ and $f_2(t)$, are determined. Applying this sequence to the actual 2-agent equations of motion described by (1), the *ideal* physical trajectories of the agents are found. This trajectory is defined as the discrete, time dependent state $\{\check{x}_i^k, \check{y}_i^k, \check{z}_i^k\}$ on the discretized interval $k = \left[1, \frac{T}{h}\right)$ for each time step, k, each agent, i, a terminal time, T, and a step size, h.

Starting with both agents at the origin and initially specifying $C_x = 0$, $C_z = 1$, $Q_{\mathbf{q}} = 0$, $Q_{\mathbf{v}} = 0$, and $Q_T = 10I$ (where I is an appropriately sized identity matrix), separation is achieved in the spanwise direction using penalty terms that only weight terminal position without regard toward the cost of intermediate input values ($Q_{\mathbf{v}}$) or state positions ($Q_{\mathbf{q}}$). Results of such idealized separation determined though MPC analysis are shown in Fig. 3.

In additional to cross-flow separation, changing the C_x separation constant allows control trajectories to be developed that separate agents in both the x and z directions (as shown

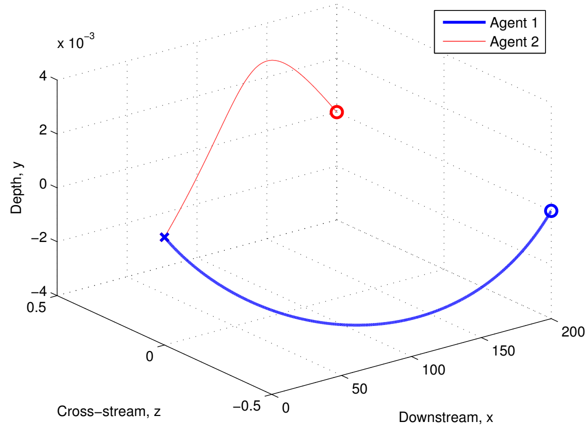

Fig. 3. Unit separation in the spanwise, z, direction of a 2-agent system subject to idealzed open channel flow. $\times$ indicates starting location and $\bigcirc$ indicates final position. Initial positions at the origin with $C_x = 0$, $C_z = 1$, $Q_{\mathbf{q}} = 0$, $Q_{\mathbf{v}} = 0$, and $Q_T = 10I$

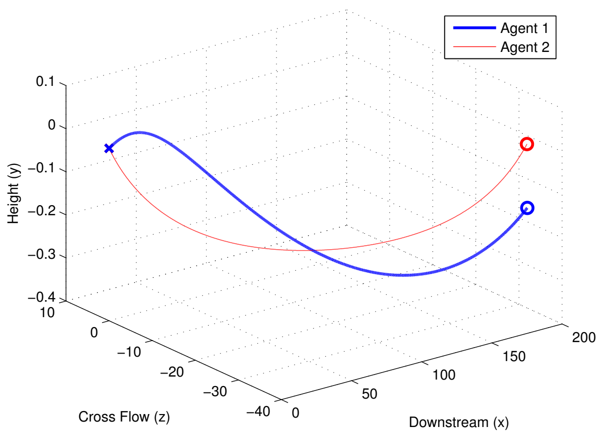

Fig. 4. Separation constants of $C_z = 1$ and $C_x = 5$, direction anof a 2-agent system subject to idealzed open channel flow. $\times$ indicates starting location and $\bigcirc$ indicates final position. Initial positions at the origin with $C_x = 0$, $C_z = 1$, $Q_{\mathbf{q}} = 0$, $Q_{\mathbf{v}} = 0$, and $Q_T = 10I$

in Fig. 4 which uses the same initial conditions as Fig. 3 but with $C_x = 5$). It is worth noting that the ideal input values do not dive the agents back to the centerline of the channel in the shown control sequence; which was already noted to be an unstable result. To correct for this problem, additional gain can be added to the control sequence (via increasing the $Q_{\mathbf{v}}$ gain matrix) which would cause the control sequence to approach as small a deivation from the centerline as possible over the trajectory window.

V. Trajectory Tracking via LQR Feedback

Under idealized circumstances, the MPC analysis of trajectory generation provides enough information to reach a local minimization of the cost function and track to a reasonable solution to the separation problem. The result, however, cannot account for variation in starting location or intermittent perturbation of the state during the actual state evolution.

The open loop controller is not enough to satisfy stability under more realistic flow parameters. Introduction of a closed-loop feedback stabilization method is necessary in order to reject disturbances in background noise and correct for variation in state position.

Using the solution to the linear-quadratic regulator (LQR) problem, an optimal control feedback gain is found which can be used to stabilize the system. In order to apply a linear feedback, the system must be linearized about the preferred state. In the 2-agent system, each agent is linearized about the ideal trajectory developed within the MPC framework.

Defining the LQR-state, $\mathcal{G}_i$, and input, $\mathcal{F}_i$, as:

$$\mathcal{G}_i \triangleq \begin{bmatrix} \breve{x}_i^1 \\ \breve{y}_i^1 \\ \breve{z}_i^1 \\ \vdots \\ \breve{x}_i^k \\ \breve{y}_i^k \\ \breve{z}_i^k \\ \vdots \\ \breve{x}_i^n \\ \breve{y}_i^n \\ \breve{z}_i^n \end{bmatrix} \Rightarrow \frac{d}{dt}\mathcal{G}_i = \begin{bmatrix} -\left(y_i^1\right)^2 + 1 \\ f_i^1 \\ \breve{y}_i^1 \\ \vdots \\ -\left(\breve{y}_i^k\right)^2 + 1 \\ f_i^k \\ \breve{y}_i^k \\ \vdots \\ -\left(\breve{y}_i^n\right)^2 + 1 \\ f_i^n \\ \breve{y}_i^n \end{bmatrix}, \quad \mathcal{F}_i \triangleq \begin{bmatrix} f_i^1 \\ \vdots \\ f_i^k \\ \vdots \\ f_i^n \end{bmatrix}, \tag{26}$$

over the sequence of ideal trajectory locations, $\{\breve{x}_i^k, \breve{y}_i^k, \breve{z}_i^k\}$, and inputs, f_i^k, for each agent derived by the MPC solution over the time sequence $t = [1, 2, ..., k, ...n]$ for $n = \frac{T}{h}$. The trajectory-linearized system is then expressed in the form $d\mathcal{G}_i/dt = A_i\mathcal{G}_i + B_i\mathcal{F}_i$, where A_i and B_i are the associated Jacobian matrices for each agent, i:

$$A_i = \begin{bmatrix} a_i^1 & 0 & \dots & 0 \\ 0 & a_i^2 & & \\ \vdots & & \ddots & \\ 0 & & & a_i^n \end{bmatrix}, \quad a_i^j = \begin{bmatrix} 0 & -2y_i^j & 0 \\ 0 & 0 & 0 \\ 0 & 1 & 0 \end{bmatrix}, \tag{27}$$

and

$$B_i = \begin{bmatrix} b_i^1 & 0 & \dots & 0 \\ 0 & b_i^2 & & \\ \vdots & & \ddots & \\ 0 & & & b_i^n \end{bmatrix}, \quad b_i^j = \begin{bmatrix} 0 \\ 1 \\ 0 \end{bmatrix}. \tag{28}$$

The feedback gain is solved via the time-dependent solution to the differential Riccati equation:

$$\frac{-dX_i}{dt} = A_i^H X_i + X_i A_i - X_i B_i Q_{\hat{f}}^{-1} B_i^H X_i + Q_X \quad \text{where} \quad X(T) = Q_{term}. \tag{29}$$

The solutions, $X = X(t)$, are determined via a backwards-in-time march using the RK4 scheme and the feedback-augmented input, $\hat{f}_i$, is given by the feedback gain, K_i, multiplied by the *difference* between the evolving actual state position given in (1) and the a vector of MPC-derived ideal state position:

$$\hat{f}_i = K_i \left(\begin{bmatrix} \breve{x}_i \\ \breve{y}_i \\ \breve{z}_i \end{bmatrix} - \begin{bmatrix} x_i \\ y_i \\ z_i \end{bmatrix} \right) \quad \text{where} \quad K_i = -Q_{\hat{f}}^{-1} B_i^H X_i. \tag{30}$$

Once again, the 'strength' of the feedback gain can be controlled via the relative magnitudes of the diagonal weighting matrices $Q_{\hat{f}}$, a weight on the cost of the input, Q_X, a weight on the intermediate perturbed state, and Q_{term}, a weight on the terminal positional variation from ideal.

The structure of the A_i and B_i matrices [(27) and 28, respectively] allow the Riccati equation to be solved as a set of $n = \frac{T}{h}$ smaller differential equations by marching the system

$$\frac{-dX_i^k}{dt} = X_i^k a_i^k + \left(a_i^k\right)^T X_i^k - X_i^k \left(b_i^k\right)^T Q_{\hat{f}}^k b_i^k X_i^k + Q x_i^k \tag{31}$$

from $t = T \rightarrow k$ for an incremented time interval $k = [0, h, 2h, ..., T-h, T]$. Then solving for the time-interval, k, dependent feedback gain, K_i^k, and input, $\hat{f}_i^k$:

$$\hat{f}_i^k = K_i^k \left(\begin{bmatrix} \breve{x}_i^k \\ \breve{y}_i^k \\ \breve{z}_i^k \end{bmatrix} - \begin{bmatrix} x_i^k \\ y_i^k \\ z_i^k \end{bmatrix} \right) \quad \text{where} \quad K_i^k = -Q_{\hat{f}}^{-1} B_i^H X_i^k. \tag{32}$$

Using this trajectory-linearized feedback control, variations in initial conditions or background velocity flows can be neutralized. This feedback effectively tracks each agent back to its MPC ideal path but adds computational cost with the one time marching of the set of systems to determine the value of K_i^k for each time interval, k.

Starting with a perturbed initial state $\{x_1 = 0, y_1 = 0, z_1 = 1\}$ and $\{x_2 = y_2 = z_2 = 0\}$, and seeking a unit separation in the cross-stream, z, direction ($C_x = 0$ and $C_z = 1$), the feedback gain successfully tracks astray agent 1 back to the ideal trajectory as shown in Fig. 5.

The feedback gain also allows intermittent background disturbance rejection. Starting with both agents at the origin and seeking unit cross-stream separation (as in Fig. 3), the agent's feedback augmented input is able to correct for the application of an additional shear term ($d\tilde{z}/dt = dz/dt + 1$) at $t = 100$ and return to the ideal path as shown in Fig. 6.

More importantly, the solution to the LQR problem provides disturbance rejection for random noise that may occur continually in the background flow and agent inputs. Modeling variation in the state velocities is achieved by augmenting (1) with scaled zero mean white noise, $w_{dx/dt}$, w_f, and $w_{dz/dt}$ at each discrete function call in the RK4 march. In this illustrative example using LQR, the added noise need not necessarily be Gaussian:

$$\frac{d}{dt} \begin{bmatrix} x_i^k \\ y_i^k \\ z_i^k \end{bmatrix} = \begin{bmatrix} -\left(y_i^k\right)^2 + 1 & + & \mathcal{X}_i^k w_{dx/dt}^k \\ f_i^k & + & \mathcal{Y}_i w_f \\ y_i^k & + & \mathcal{Z}_i^k w_{dz/dt}^k \end{bmatrix}. \tag{33}$$

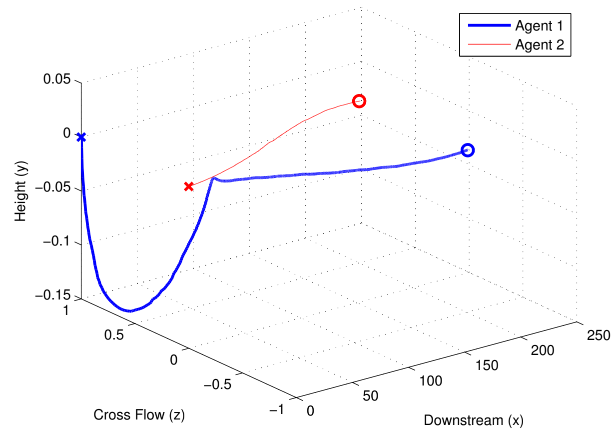

Fig. 5. Trajectory tracking for a perturbed initial state with ideal trajectories seeking unit separation in the spanwise, z, direction of a 2-agent system subject to idealized channel flow. $\times$ indicates starting location and $\bigcirc$ indicates final position. Initial position $\{x_1 = 0, y_1 = 0, z_1 = 1\}$ and $\{x_2 = 0, y_2 = 0, z_2 = 0\}$ with $C_x = 0$, $C_z = 1$, $Q_{\mathbf{q}} = 0$, $Q_{\mathbf{v}} = 0$, and $Q_T = 10I$

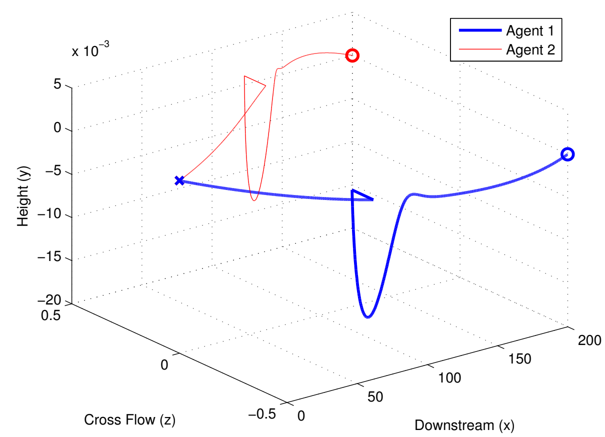

Fig. 6. Trajectory tracking for an intermittently excited background flow with ideal trajectories seeking unit separation in the spanwise, z, direction of a 2-agent system subject to idealized channel flow. $\times$ indicates starting location and $\bigcirc$ indicates final position. Initial positions at the origin with $C_x = 0$, $C_z = 1$, $Q_{\mathbf{q}} = 0$, $Q_{\mathbf{v}} = 0$, and $Q_T = 10I$

The scaling factors, $\mathcal{X}_i^k = -\left(y_i^k\right)^2 + 1$ and $\mathcal{Z}_i^k = y_i^k$, are used to ensure that the maximum value of the noise term is the same size as the ideal background flow at the particular depth y_i^k. Scaling in the vertical velocity, dy/dt, is done with a constant such that $\mathcal{Y}_i = \max \mathcal{F}_i$ for the input sequence, $\mathcal{F}_i$, determined via (26).

Applying such a scaled noise to background flow and agent input, the feedback gain is sufficiently powerful to continually adapt the input sequence of each agent so as to draw it back to the ideal MPC trajectory as shown in Fig. 7.

VI. Conclusions

The use of buoyancy controlled agent motion, in conjunction with a known stratified background flow environ-

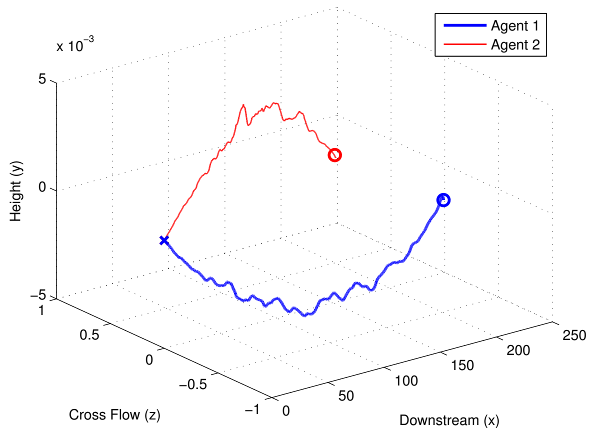

Fig. 7. Trajectory tracking for a scaled zero mean white noise excited background flow with ideal trajectories seeking unit separation in the spanwise, z, direction of a 2-agent system subject to idealized open channel flow. $\times$ indicates starting location and $\bigcirc$ indicates final position. Initial positions at the origin with $C_x = 0$, $C_z = 1$, $Q_{\mathbf{q}} = 0$, $Q_{\mathbf{v}} = 0$, and $Q_T = 10I$

ment, provides enough control authority to create separation between several agents in the same flow. Several types of background flow can be similarly characterized, and calculated solutions to the control problem uniquely mapped back to form different physical solutions under the same mathematical guise.

Limited to a defined time window, an iterative approach is used to solve the general separation problem. Defining an adjoint of the agent state as presented in (25a), a gradient of the cost function with respect to the current input is determined in (10). Using a descent method to determine an appropriate step size, the cost function is minimized by moving the input, $\mathbf{v}$, by the resultant step size and direction. The process is repeated as necessary to ensure convergence of the function, J, to a local minimum.

The solution to the MPC problem (11) is a vector of inputs to the COV system, $\mathbf{v}$, which minimize the desired cost function. This resultant COV input is then mapped back to the desired background flow, via (8), and a sequence of actual agent inputs is recovered. Under the ideal background flow considered in the mathematical construction of the MPC problem in (1), this input results in the desired spacing of the agents in the streamwise and spanwise directions. This solution works under an idealized background flow, is purely open loop, and has no disturbance rejection capability.

By linearizing the state of each agent about its MPC-derived ideal trajectory as done in (27) and (28), a feedback gain is calculated by solving the differential Riccati equation presented in (29) and (32). Augmenting the MPC-derived input via this LQR gain, perturbed system states, variation in starting locations, and intermittent noise in background flows are corrected for within the original trajectory time-frame (Figs. 5, 6, and 7 respectively).

VII. Future Work

The major cost of the presented MPC calculation is the Runge-Kutta march of the state and adjoint over the time window. Each iteration of the cost function optimization involves both a full state and a full adjoint march over the window in order to produce a gradient. Therefore, it is important that the numerical processes associated with the cost function minimization presented in Eqs. 10-25 limit, as much as possible, the required number steps to reach a minimum value.

While the conjugate gradient descent method in conjunction with a Brent line search method is adequate, it can require a large number of function calls and be computationally expensive. There are several numerical methods of interest, notably variations on reduced memory versions of the Broyden-Fletcher-Goldfarb-Shanno (BFGS) descent method [7], which have been shown in preliminary results require substantially fewer function evaluations under similar minimization accuracy constraints.

The current formulation of the LQR feedback is based on the assumption of perfect state knowledge. Relaxing this assumption, a linear-quadratic Gaussian (LQG) controller can be formulated by modeling using the Kalman estimate in place of the state in the LQR problem formulation [6].

Using direct numerical simulation of incompressible Navier-Stokes, simulations with equivalent flow structures to the ideal case presented in (1) can be applied ranging from laminar flow to fully turbulent mixing. Applying the MPC/LQG framework to these more complicated flows will give greater understanding of both the time window needed for separation and the relative weightings of all the control parameters. This, in turn, forms the basis for expanding the flow field beyond the channel limitations, and applying the method to full oceanic/atmospheric flow fields.

VIII. Acknowledgements

The authors would like to thank Paul Belitz, Joseph Cessna, Christopher Colburn, and David Zhang for helpful discussions related to this work.

References

[1] Davis, R. E. (1991) Lagrangian Ocean Studies. *Annual Review of Fluid Mechanics*, vol. 23, pp. 43-64.

[2] Businger, S., R. Johnson & Talbot (2006) Scientific Insights from Four Generations of Lagrangian Balloons in Atmospheric Research. *Bulletin of the American Meteorology Society* vol. 87, no. 11, pp. 1539-1554.

[3] Soeterboek, R. (1992) Predictive Control: a Unified Approach. Prentice Hall.

[4] Bitmead, R. R., M. Gevers, & V. Wertz (1990) Adaptive Optimal Control: The Thinking Mans GPC. Prentice Hall.

[5] Bewley, T., P. Moin & R. Temam (2001) DNS-based predictive control of turbulence: an optimal benchmark for feedback algorithms. *Journal of Fluid Mechanics*, vol. 447, pp. 179-225.

[6] Fortmann, T. & K. Hitz (1977) An Introduction to Linear Control Systems. Mercel Dekker, Inc.

[7] Gill P. E. & M. W. Leonard (2003) Limited-Memory Reduced-Hessian Methods for Large-Scale Unconstrained Optimization. *SIAM Journal on Optimization*, vol. 14, issue 2, pp. 380-401.